

# A New $^{17}\text{F}(p,\gamma)^{18}\text{Ne}$ Reaction Rate and Its Implications for Nova Nucleosynthesis

S. Parete-Koon<sup>1,2</sup>, W. R. Hix<sup>1,2,3</sup>, M.S. Smith<sup>2</sup>, S. Starrfield<sup>4</sup>, D.W. Bardayan<sup>2</sup>, M.W. Guidry<sup>1,2</sup>, A. Mezzacappa<sup>2</sup>

## ABSTRACT

Proton capture by  $^{17}\text{F}$  plays an important role in the synthesis of nuclei in nova explosions. A revised rate for this reaction, based on a measurement of the  $^1\text{H}(^{17}\text{F},p)^{17}\text{F}$  excitation function using a radioactive  $^{17}\text{F}$  beam at ORNL's Holifield Radioactive Ion Beam Facility, is used to calculate the nucleosynthesis in nova outbursts on the surfaces of 1.25  $M_{\odot}$  and 1.35  $M_{\odot}$  ONeMg white dwarfs and a 1.00  $M_{\odot}$  CO white dwarf. We find that the new  $^{17}\text{F}(p,\gamma)^{18}\text{Ne}$  reaction rate changes the abundances of some nuclides (e.g.,  $^{17}\text{O}$ ) synthesized in the hottest zones of an explosion on a 1.35  $M_{\odot}$  white dwarf by more than a factor of  $10^4$  compared to calculations using some previous estimates for this reaction rate, and by more than a factor of 3 when the entire exploding envelope is considered. In a 1.25  $M_{\odot}$  white dwarf nova explosion, this new rate changes the abundances of some nuclides synthesized in the hottest zones by more than a factor of 600, and by more than a factor of 2 when the entire exploding envelope is considered. Calculations for the 1.00  $M_{\odot}$  white dwarf nova show that this new rate changes the abundance of  $^{18}\text{Ne}$  by 21%, but has negligible effect on all other nuclides. Comparison of model predictions with observations is also discussed.

*Subject headings:* nuclear reactions, nucleosynthesis, novae

## 1. Introduction

Nova explosions result from the transfer of stellar material onto a white dwarf star (WD) from a companion star. The mass transfer and resulting rise in temperature initiate hydrogen

---

<sup>1</sup>Department of Physics & Astronomy, University of Tennessee, Knoxville, Tennessee 37996-1200

<sup>2</sup>Physics Division, Oak Ridge National Laboratory, Oak Ridge, TN 37831-6354

<sup>3</sup>Joint Institute For Heavy Ion Research, Oak Ridge National Laboratory, Oak Ridge, Tennessee 37831-6374

<sup>4</sup>Department of Physics & Astronomy, Arizona State University, Tempe, AZ 85287-1504

burning via the CNO cycle and trigger a violent thermonuclear explosion on the WD surface providing an energy release of up to  $\sim 10^{46}$  ergs with the peak of the thermonuclear runaway lasting up to 1000 seconds and the observed outburst lasting years (Gehrz et al. 1998). These outbursts are the largest hydrogen driven thermonuclear explosions in the Universe, and are characterized by high temperatures and densities in the nuclear burning region - greater than  $10^8$  K and  $10^4$  g cm $^{-3}$ , respectively (Starrfield et al. 1978).

Under such conditions, proton and  $\alpha$  particle capture reactions on proton-rich radioactive nuclei become faster than  $\beta^+$  decays. Unstable nuclei produced by capture reactions can then undergo further reactions before they decay, resulting in a sequence of reactions (the rapid proton capture process, or *rp*-process) that is very different from the sequences in non-explosive environments (Wallace & Woosley 1981). This explosive hydrogen burning generates energy up to 100 times faster than in the quiescent burning phase and drives the outburst. The timescale for these nuclear reactions is comparable to that of convection in the exploding envelope (Starrfield 1989; Shankar & Arnett 1994), allowing the mixing of unstable nuclei into the outer envelope of the nova. For these reasons, accurate determinations of the rates of reactions on proton-rich radioactive nuclei are vitally important to our understanding of these explosions (Wiescher et al. 1998; José et al. 1999).

In addition to driving the outburst, nuclear reactions in novae can synthesize nuclides up to mass  $A \sim 40$ , producing an abundance pattern distinct from that in CNO burning in quiescent stars (Vanlandingham et al. 1996; Chin et al. 1999). For example, long-lived radioactive nuclei such as  $^{18}\text{F}$  are synthesized and ejected. Because of its relatively long half-life and significant abundance, it has been suggested that the decay of  $^{18}\text{F}$  in the nova ejecta produces the majority of observable gamma rays during the first several hours after the explosion (Harris et al. 2001). The observation of such gamma rays may provide a rather direct test of nova models (Leising & Clayton 1987; Harris et al. 1999; Hernanz et al. 1999). However, the quantity of  $^{18}\text{F}$  produced in the interior and transported to the top of the nova envelope is severely constrained by the nuclear reactions that create and destroy  $^{18}\text{F}$ . The sensitivity required to make gamma-ray observations with orbital detectors (e.g., INTEGRAL, see Hernanz et al. 2001) is therefore impossible to determine without a better understanding of the reactions that create and destroy  $^{18}\text{F}$ . Whereas the  $^{18}\text{F}(p,\alpha)^{15}\text{O}$  reaction rate is the primary destruction mechanism of  $^{18}\text{F}$  (Coc et al. 2000),  $^{18}\text{F}$  can be produced via two different reaction sequences:  $^{17}\text{F}(p,\gamma)^{18}\text{Ne}(\beta^+\nu)^{18}\text{F}$  and  $^{17}\text{O}(p,\gamma)^{18}\text{F}$ . We pay particular attention to the changes in  $^{18}\text{F}$  production arising from a newly calculated  $^{17}\text{F}(p,\gamma)^{18}\text{Ne}$  reaction rate.

## 2. The $^{17}\text{F}(\text{p},\gamma)^{18}\text{Ne}$ Reaction

Wiescher et al. (1998) suggested that the  $^{17}\text{F}(\text{p},\gamma)^{18}\text{Ne}$  reaction rate could influence the amount of  $^{15}\text{O}$ ,  $^{17}\text{F}$ ,  $^{18}\text{Ne}$ , and  $^{18}\text{F}$  produced in novae. This reaction is also part of a sequence of reactions providing a possible transition from hot CNO cycle burning to the  $rp$ -process in the most energetic novae (Wallace & Woosley 1981). An unnatural parity ( $J^\pi = 3^+$ ) state in  $^{18}\text{Ne}$  provides an  $\ell = 0$  resonance in  $^{17}\text{F} + \text{p}$  capture which was thought to dominate the  $^{17}\text{F}(\text{p},\gamma)^{18}\text{Ne}$  reaction rate at nova temperatures (Wiescher et al. 1988). This level was expected from the structure of the  $^{18}\text{O}$  isobaric mirror nucleus, but never conclusively observed despite nine experimental studies of the relevant excitation energy region in  $^{18}\text{Ne}$ . Different determinations of the properties (excitation energy, total width) of this level - based on shell model calculations - resulted in differences of more than a factor of 100 in the  $^{17}\text{F}(\text{p},\gamma)^{18}\text{Ne}$  reaction rate (Wiescher et al. 1988; García et al. 1991; Sherr & Fortune 1998). The rate used in REACLIB (Thielemann et al. 1995), the reaction rate library most widely-used for nova simulations, is that of Wiescher et al. (1988), which is the fastest rate primarily because their estimate of the excitation energy for the  $J^\pi = 3^+$   $^{18}\text{Ne}$  resonance was the lowest.

A measurement of the excitation function for the  $^1\text{H}(^{17}\text{F},\text{p})^{17}\text{F}$  reaction at ORNL’s Holifield Radioactive Ion Beam Facility (HRIBF) was used to obtain the first unambiguous evidence for the  $J^\pi = 3^+$  state in  $^{18}\text{Ne}$  and precisely determine its energy and total width (Bardayan et al. 1999). Using a calculation of the (still unmeasured)  $\gamma$ -width of this level, its contribution to the  $^{17}\text{F}(\text{p},\gamma)^{18}\text{Ne}$  reaction rate (Bardayan et al. 2000) was determined, thereby resolving the greatest uncertainty in the  $^{17}\text{F}(\text{p},\gamma)^{18}\text{Ne}$  reaction rate. Combining this measurement with calculations of the non-resonant direct capture rate from García et al. (1991), the  $J^\pi = 3^+$  level is now estimated to only dominate the capture rate at temperatures above  $5 \times 10^8$  K, while direct capture dominates at the lower temperatures ( $\lesssim 4 \times 10^8$  K) characteristic of novae. A parameterization of this reaction rate is given in the REACLIB format in Bardayan et al. (2000). To explore the astrophysical impact of the ORNL measurement (Bardayan et al. 1999), which only influences the resonant reaction rate, we constructed four different reaction rates for our study - based on the direct capture rate from GAM91 added to the resonant rate using parameters from Wiescher et al. (1988); García et al. (1991); Sherr & Fortune (1998); Bardayan et al. (1999). Hereinafter, we will refer to these as the WGT88, GAM91, SF98, and ORNL rates, respectively. The ratios of the ORNL  $^{17}\text{F}(\text{p},\gamma)^{18}\text{Ne}$  reaction rate to the other three rates are shown in Figure 1. At nova temperatures ( $\sim 0.1 - 0.4$  GK), the new ORNL rate differs only slightly from the SF98 and GAM91 rates, but differs by up to a factor of 30 from the rate based on the WGT88 resonance parameters. These latter parameters are the basis for the rate in the widely-used REACLIB reaction rate library.

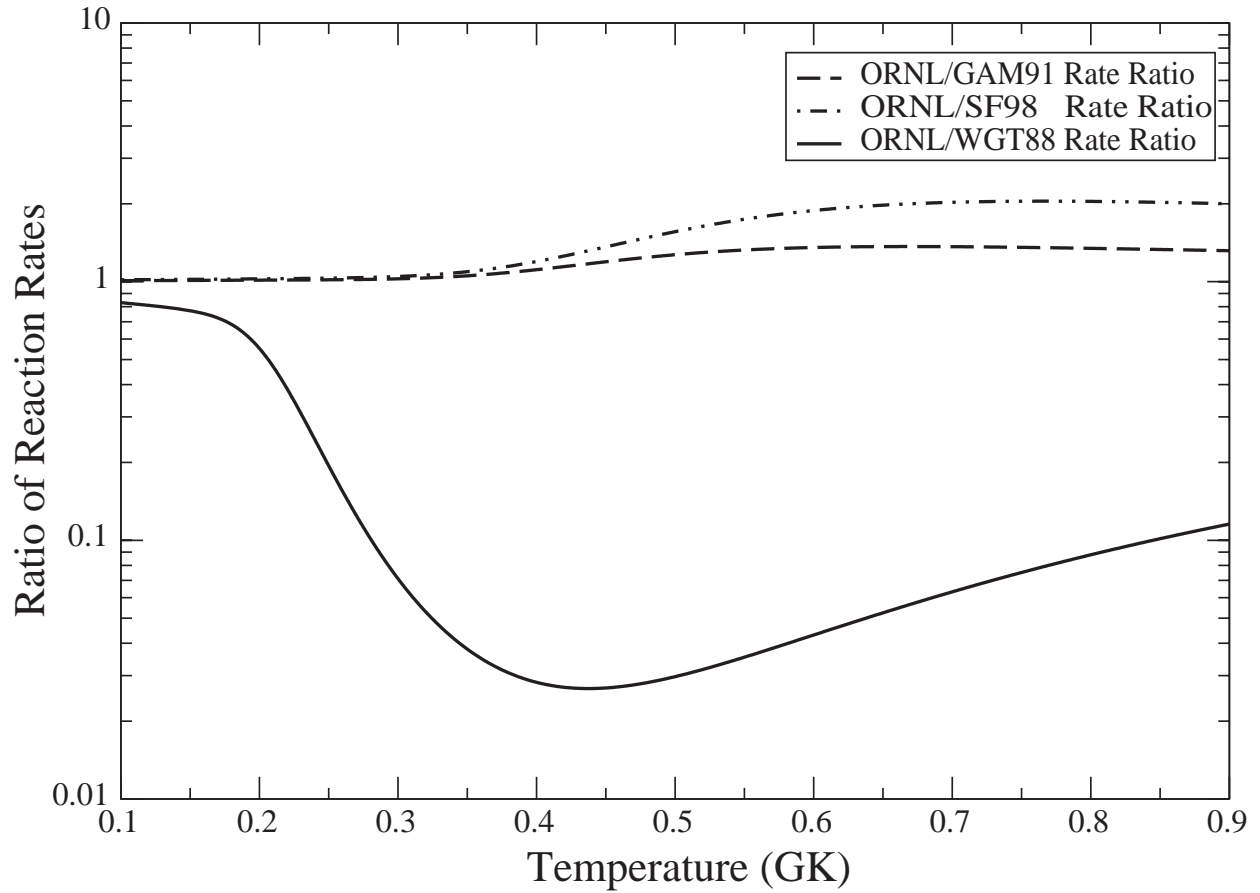


Fig. 1.— Ratio of the new ORNL  $^{17}\text{F}(p,\gamma)^{18}\text{Ne}$  rate (Bardayan et al. 2000) to three previous estimates, WGT88 (Wiescher et al. 1988), SF98 (Sherr & Fortune 1998), and GAM91 (García et al. 1991), as a function of stellar temperature. The temperature range of interest for novae is approximately 0.1-0.4 GK.

### 3. Nova Nucleosynthesis Calculations

The temporal evolution of the isotopic composition in these nova explosions was followed using a nuclear reaction network (Hix & Thielemann 1999) containing 169 isotopes, from hydrogen to  $^{54}\text{Cr}$  with nuclear reaction rates drawn from REACLIB (Thielemann et al. 1995). In this paper we examine the nucleosynthesis of 3 models for nova explosions, on a  $1.00 M_{\odot}$  CO WD, on a  $1.25 M_{\odot}$  ONeMg WD, and on a  $1.35 M_{\odot}$  ONeMg WD. The first two are representative of the most prevalent classes of novae, while the third represents a more energetic outburst. Thirty to fifty per cent of all novae are thought to occur on ONeMg white dwarfs (Gehrz et al. 1998; Gil-Pons et al. 2003).

In many prior nucleosynthesis calculations, the nuclear reaction network was evolved under conditions of constant temperature and density (e.g., Champagne & Wiescher 1992; Van Wormer et al. 1994). This neglects the strong coupling of the nucleosynthesis to the hydrodynamics. This coupling is important because the nuclear reactions generate the energy powering the outburst, and the reaction rate between any two nuclear species is highly variable in time due to its dependence on the temperature and density. A fully consistent description of an outburst therefore involves the coupling of a large reaction network with a multidimensional hydrodynamic calculation of the outburst, an approach which is made computationally demanding by the similar timescales of the nuclear reactions and convective motions in novae. However, such simulations are in their infancy (Shankar & Arnett 1994; Kercek et al. 1999).

We have improved on constant temperature and density nucleosynthesis calculations by extracting hydrodynamic trajectories – time histories of the temperature and density – from one-dimensional hydrodynamic calculations for outbursts on  $1.0$ ,  $1.25$ , and  $1.35 M_{\odot}$  white dwarfs (similar to those of Starrfield et al. 1998) which employed a more limited reaction rate network. Different mass elements (*zones*) of the envelope at different radii generate unique trajectories. For example, the temperature history of the hottest zone of the  $1.25 M_{\odot}$  ONeMg WD nova appears later in Figure 4. In our simulations, the ejecta of each of the nova models consisted of between 26 and 31 zones. Separate *post-processing* nuclear reaction network calculations with the full complement of nuclei and nuclear reactions were carried out to study the nucleosynthesis details within each zone; no mixing between the zones was included. To calculate the total abundances in the ejecta of each explosion, a sum was made of abundances over the zones, weighted by the ratio of the zone mass to the total envelope mass. It should be noted that calculations of nova outbursts on similar WD progenitors carried out by different groups (e.g., José et al. 1999; Wanaajo et al. 1999) have yielded moderately different hydrodynamic trajectories (and peak temperatures) .

The calculations for the  $1.25 M_{\odot}$  and  $1.35 M_{\odot}$  ONeMg WD novae begin with a set of

initial abundances adopted from Politano et al. (1995). They assumed a solar composition mixed equally (by mass) with the ashes of carbon burning (50%  $^{20}\text{Ne}$ , 30%  $^{16}\text{O}$ , and 20%  $^{24}\text{Mg}$ ). The initial composition for the  $1.00 M_{\odot}$  CO WD nova was 50% solar (Anders & Grevesse 1989) (by mass) and 50% products of He burning (an equal mix of  $^{12}\text{C}$  and  $^{16}\text{O}$  with a trace of  $^{22}\text{Ne}$ ). The composition in each case is representative of the envelope material mixing with the matter from the underlying white dwarf (Starrfield et al. 1974).

To see the effect of the  $^{17}\text{F}(p,\gamma)^{18}\text{Ne}$  reaction rate on the nucleosynthesis, this post-processing nucleosynthesis calculation was run for each nova model with each of the reaction rates, those based on resonance parameters from ORNL (Bardayan et al. 1999), WGT88 (Wiescher et al. 1988), SF98 (Sherr & Fortune 1998), and GAM91 (García et al. 1991), substituted into the reaction rate library. In each calculation, the only reaction rates changed in the library are the  $^{17}\text{F}(p,\gamma)^{18}\text{Ne}$  reaction rate and its inverse (obtained via detailed balance). At late times in the outburst, the adiabatic expansion drops the temperatures of the ejecta below  $10^7$  K, where only the weak reactions significantly change the nuclear abundances. Additionally, the reaction rate parameters compiled in REACLIB (Thielemann et al. 1995) are valid only from  $10^7$  K to  $10^{10}$  K. For these reasons, while the complete set of reactions was used to evolve the abundances for temperatures in excess of  $10^7$  K, only the weak reactions were used at lower temperatures. The simulations were stopped one hour after the peak temperature was reached in the hottest zone so that the potentially observable abundances of long-lived radionuclides (e.g.,  $^{18}\text{F}$ ) could be determined. Our analysis of the impact of the new  $^{17}\text{F}(p,\gamma)^{18}\text{Ne}$  reaction rate was, however, insensitive to the stop time.

For each nova, the abundance pattern produced by the network calculations with the ORNL  $^{17}\text{F}(p,\gamma)^{18}\text{Ne}$  rate was compared to the abundance pattern produced by the network calculations done with the other  $^{17}\text{F}(p,\gamma)^{18}\text{Ne}$  rates. This analysis was performed for each zone individually and for a weighted sum of all zones. Particular scrutiny was given to the influence of the new  $^{17}\text{F}(p,\gamma)^{18}\text{Ne}$  reaction rate on the production of the potentially observable radioisotope  $^{18}\text{F}$ . Careful attention was also paid to the changes in nuclear energy generation resulting from changing the  $^{17}\text{F}(p,\gamma)^{18}\text{Ne}$  reaction rate. The post-processing approach used to calculate the nucleosynthesis is valid as long as changes to the reaction rate library result in negligible changes in the energy production, and therefore would not alter the temperature and density history of the explosion. The hydrodynamic profiles were generated by a network which used the WGT88 rate for the  $^{17}\text{F}(p,\gamma)^{18}\text{Ne}$  rate. We compared the energy generation of the calculations with the ORNL, SF98 and GAM91 rates to the energy generation by the calculation with the WGT88 rate. For the  $1.25 M_{\odot}$  WD nova, the calculations with the ORNL, SF98 and GAM91 rates showed less than 1% difference in energy generation from the calculation with the WGT88 rate for the entire exploding envelope and 2.13%, 2.21%, and 2.18% difference, respectively, for the hottest zone. For the

1.35  $M_{\odot}$  WD, the ORNL, SF98, and GAM91 rates resulted in energy generation differences of 1.02%, 1.10%, and 1.06% for the sum of all zones and 0.02%, 0.08%, and 0.05%, respectively, for the hottest zone compared to energy generation resulting from the WGT88 rate. There was less than 0.01% difference between the energy generation for rates in the 1.00  $M_{\odot}$  WD nova calculations. From these results, we conclude that our rate variations cause a negligible change in the temperature and density of the explosion, verifying the validity of our post-processing nucleosynthesis calculations.

#### 4. Results for a 1.25 $M_{\odot}$ ONeMg WD Nova

Comparisons between the mass fractions calculated with the ORNL and WGT88 rates show the largest changes for the nuclides  $^{18}\text{F}$  (ORNL/WGT88 mass fraction ratio = 2.08),  $^{18}\text{O}$  (2.00),  $^{17}\text{O}$  (1.92),  $^{17}\text{F}$  (1.77),  $^{14}\text{C}$  (1.39),  $^{14}\text{N}$  (0.776),  $^{14}\text{O}$  (0.745),  $^{13}\text{C}$  (0.702),  $^{15}\text{O}$  (0.629),  $^{15}\text{N}$  (0.542), and  $^{19}\text{F}$  (0.433), when all zones of the nova were considered (Figure 2). A comparison of the mass fractions from the hottest zone (Figure 3), which contains  $\sim 16\%$  of the total mass of the envelope and where the largest number of the nuclear transmutations occur, shows the largest changes for  $^{18}\text{F}$  (ORNL/WGT88 mass fraction ratio = 604),  $^{18}\text{O}$  (604),  $^{17}\text{O}$  (559),  $^{17}\text{F}$  (527),  $^{19}\text{F}$  (3.5), and  $^3\text{He}$  (0.43).

The simple expectation is that the network with the faster  $^{17}\text{F}(\text{p},\gamma)^{18}\text{Ne}$  rate would produce more  $^{18}\text{F}$  because this nuclide is the direct decay product of  $^{18}\text{Ne}$ . This is the case for the cooler outer regions of these nova, where the lower temperatures do not allow a high probability for  $^{18}\text{F}$  destruction via  $^{18}\text{F}(\text{p},\alpha)^{15}\text{O}$ . Thus the early surplus of  $^{18}\text{F}$  production caused by the faster  $^{17}\text{F}(\text{p},\gamma)^{18}\text{Ne}$  rate is maintained as the envelope cools. This is not, however, the case for the hotter inner zones where most of the nucleosynthesis occurs. Calculations with the faster  $^{17}\text{F}(\text{p},\gamma)^{18}\text{Ne}$  rate do produce an early surplus of  $^{18}\text{F}$  in these zones, but at times when the temperatures are high. This allows the  $^{18}\text{F}(\text{p},\alpha)^{15}\text{O}$  reaction to destroy this surplus, though convective mixing to cooler layers may preserve some of this surplus.

Models with the slower  $^{17}\text{F}(\text{p},\gamma)^{18}\text{Ne}$  rates produce more  $^{18}\text{F}$  in the hotter, inner zones (via  $^{17}\text{F}(\beta^+\nu)^{17}\text{O}(\text{p},\gamma)^{18}\text{F}$ , leading to a larger amount of  $^{18}\text{F}$  when averaged over the entire envelope. This can be seen in Figure 4 which shows the time evolution of several abundances in the hotter, innermost ejecta zone of the 1.25  $M_{\odot}$  WD nova. There are two reaction paths that lead from  $^{17}\text{F}$  to  $^{18}\text{F}$ :  $^{17}\text{F}(\text{p},\gamma)^{18}\text{Ne}(\beta^+\nu)^{18}\text{F}$  and  $^{17}\text{F}(\beta^+\nu)^{17}\text{O}(\text{p},\gamma)^{18}\text{F}$ . Figure 4 shows that for 5 seconds after the time of peak temperature, the abundance of  $^{18}\text{F}$  is larger for the WGT88 case which has the faster  $^{17}\text{F}(\text{p},\gamma)^{18}\text{Ne}$  rate. This case also produces more  $^{18}\text{Ne}$ , demonstrating that the production of  $^{18}\text{F}$  is dominated by  $^{17}\text{F}(\text{p},\gamma)^{18}\text{Ne}(\beta^+\nu)^{18}\text{F}$  during

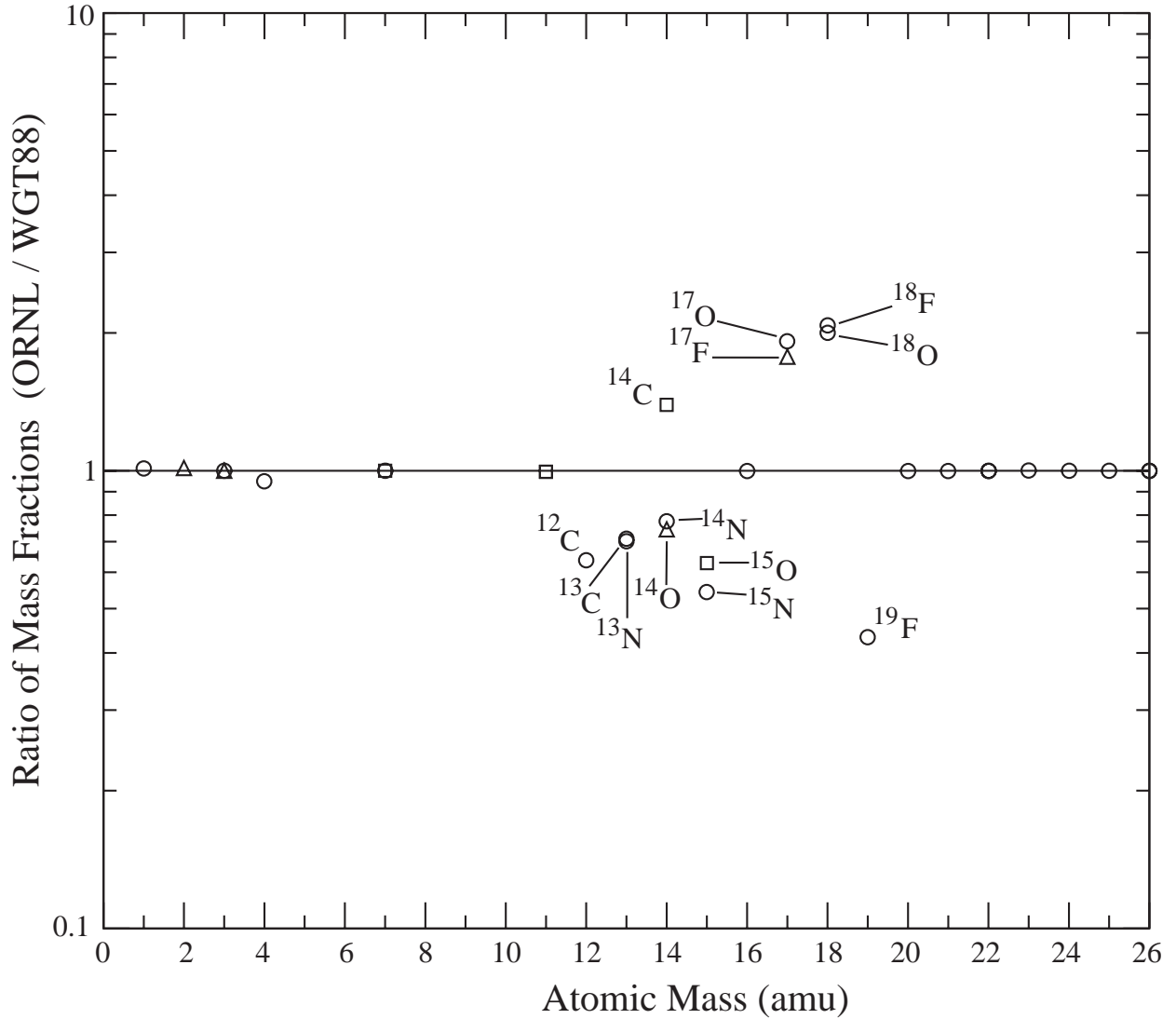


Fig. 2.— The ratio of mass fractions (ORNL/WGT88) plotted against nuclide mass for the entire envelope of a  $1.25 M_{\odot}$  WD nova. The ORNL rate changes the mass fractions of some nuclei by up to a factor of 2. The circular symbols mark species with mass fractions greater than  $10^{-8}$ , the square symbols mass fractions between  $10^{-8}$  and  $10^{-16}$ , and the triangular symbols mass fractions less than  $10^{-24}$ .

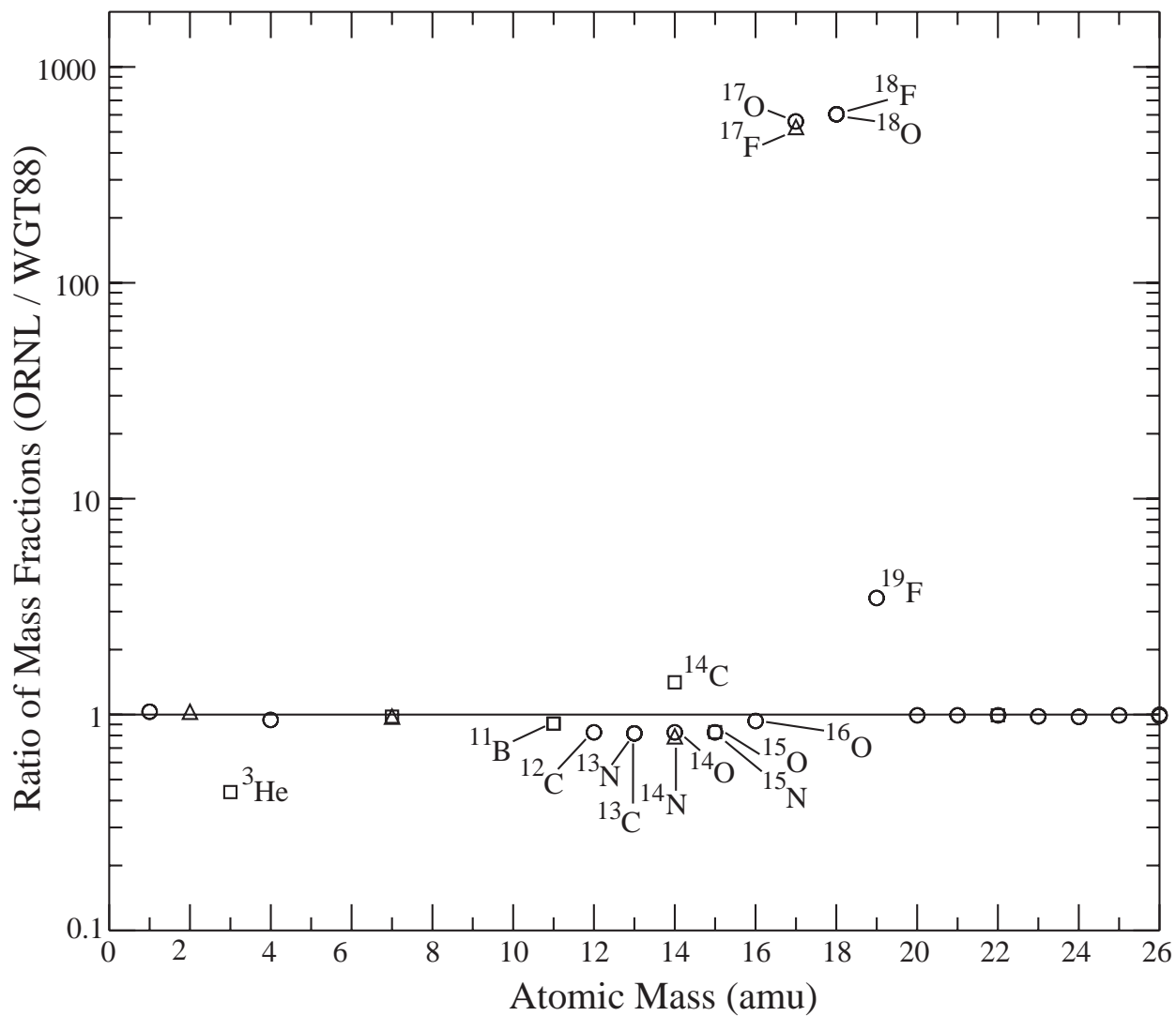


Fig. 3.— The ratio of mass fractions (ORNL/WGT88) plotted as a function of the nuclide mass for the hottest zone of a  $1.25 M_{\odot}$  WD nova. The ORNL rate changes the mass fractions of some nuclei by up to a factor of 600. The different symbols represent the same abundance levels as in Figure 2.

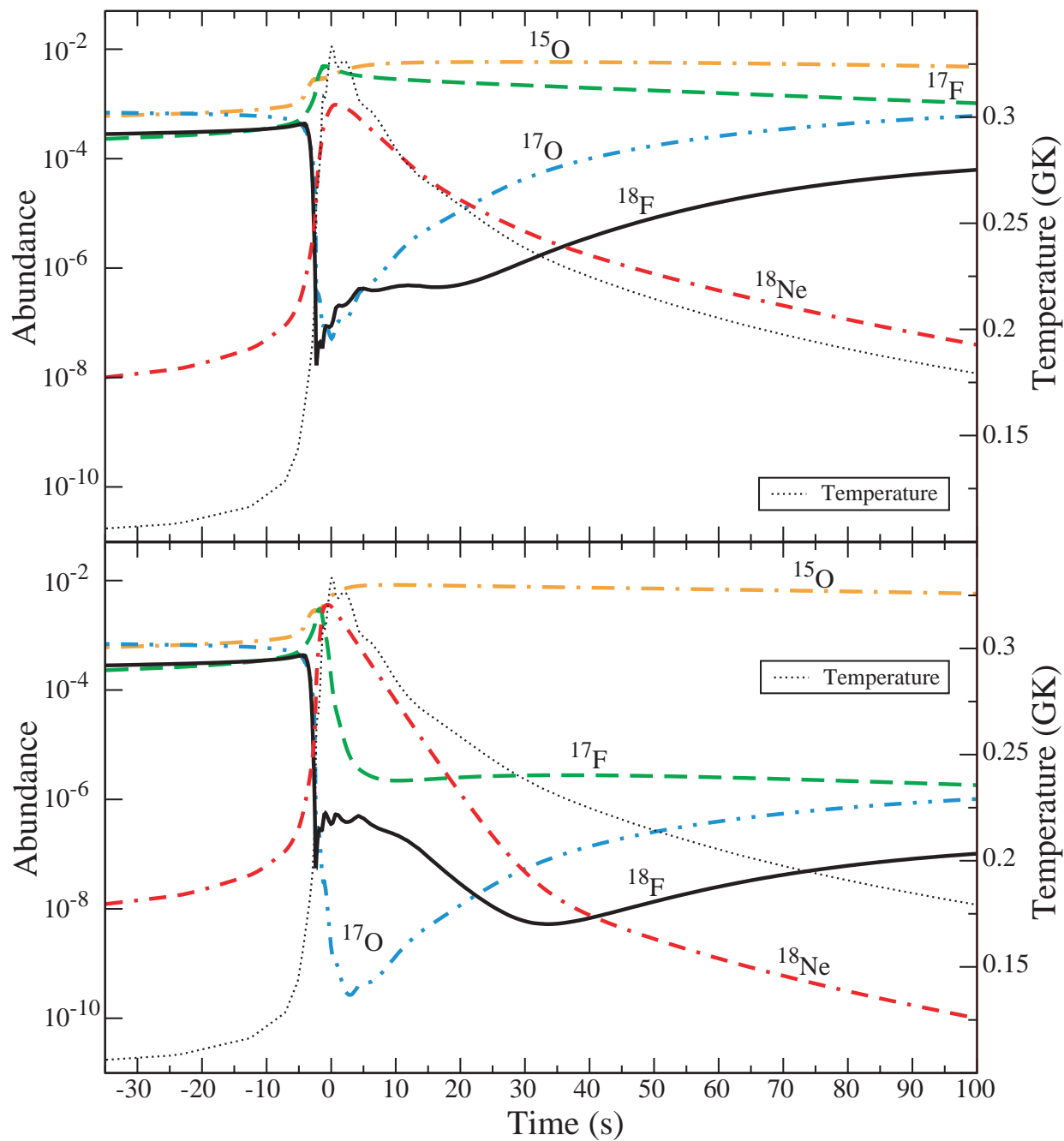


Fig. 4.— Abundances plotted as a function of time for the hottest zone of the  $1.25 M_{\odot}$  WD nova. The abundances calculated by the network with the new, slower ORNL  $^{17}\text{F}(p,\gamma)^{18}\text{Ne}$  rate are shown in (a) and the abundances calculated with the older, faster  $^{17}\text{F}(p,\gamma)^{18}\text{Ne}$  WGT88 rate are shown in (b). The temperature history for this zone is also plotted.

this period. However, the highest temperatures of the nova occur during this period, leading to further processing of the freshly-synthesized  $^{18}\text{F}$ . The faster  $^{17}\text{F}(p,\gamma)^{18}\text{Ne}$  rate does allow more transmutations from  $^{17}\text{F}$  to  $^{18}\text{F}$ , but the  $^{18}\text{F}$  is soon destroyed, primarily via the  $^{18}\text{F}(p,\alpha)^{15}\text{O}$  reaction. The network with the faster WGT88  $^{17}\text{F}(p,\gamma)^{18}\text{Ne}$  rate shows 62% more  $^{15}\text{O}$  production compared to the network with the slower rate (ORNL case) 5 seconds after peak.

The final abundance of  $^{17}\text{F}$  and  $^{17}\text{O}$  produced in the ORNL case is greater than the abundance of  $^{17}\text{F}$  and  $^{17}\text{O}$  produced in the WGT88 case because the slower  $^{17}\text{F}(p,\gamma)^{18}\text{Ne}$  ORNL rate allows more  $^{17}\text{F}$  to survive and decay to  $^{17}\text{O}$ . Beginning  $\sim 20\text{--}30$  seconds after the time of peak temperature, the abundance of  $^{17}\text{O}$  becomes greater than the abundance of  $^{18}\text{Ne}$ , allowing production of  $^{18}\text{F}$  to be dominated by the reaction sequence  $^{17}\text{F}(\beta^+\nu)^{17}\text{O}(p,\gamma)^{18}\text{F}$ . Graphically this can be seen in Figure 4 by noting that the time evolution of the  $^{18}\text{F}$  and  $^{17}\text{O}$  abundances are parallel after the  $^{18}\text{Ne}$  abundance drops below the  $^{17}\text{O}$  abundance. This figure also shows that the ORNL case starts this period with 300 times more  $^{17}\text{F}$  and  $^{17}\text{O}$  than the WGT88 case. In this period, there is little change in the abundance of  $^{15}\text{O}$  because the temperature has dropped, inhibiting the destruction of  $^{18}\text{F}$  via the  $^{18}\text{F}(p,\alpha)^{15}\text{O}$  reaction. Thus the slower  $^{17}\text{F}(p,\gamma)^{18}\text{Ne}$  rate produces a larger final abundance of  $^{18}\text{F}$  than the faster rate because the delayed production of  $^{18}\text{F}$  to the cooler post-peak temperatures allows  $^{18}\text{F}$  to survive as  $^{18}\text{F}$  and its decay product  $^{18}\text{O}$ .

The SF98 and GAM91  $^{17}\text{F}(p,\gamma)^{18}\text{Ne}$  reaction rates are, respectively, only 12% and 8% smaller than the ORNL rate at the peak temperatures of the  $1.25 M_{\odot}$  WD nova. Our calculations show that there are only small differences in the mass fractions calculated with networks containing these three rates. The largest changes, when all zone are considered, are between the SF98 and ORNL cases:  $-1.5\%$   $^{14}\text{O}$ ,  $-1.3\%$   $^{18}\text{F}$ ,  $-1.3\%$   $^{18}\text{O}$ ,  $-1.0\%$   $^{17}\text{F}$ , and  $+1.1\%$   $^{19}\text{F}$  when the ORNL rate is used. For the hottest zone, calculations with the ORNL rate result in 6.5% less  $^{17}\text{F}$ , 3.5% less  $^{18}\text{F}$  and  $^{18}\text{O}$ , 3.4% less  $^{17}\text{O}$ , 2.4% less  $^{17}\text{F}$ , and 2.0% more  $^{14}\text{O}$  compared to calculation using the SF98 rate. Comparison of calculation using the GAM91 and ORNL rates show changes of  $-0.7\%$   $^{18}\text{F}$  and  $^{18}\text{O}$  and  $+0.6\%$   $^{19}\text{F}$  in the ORNL case for the weighted sum of all zones in the  $1.25 M_{\odot}$  WD nova model. For the hottest zone, calculations using the ORNL rate result in 2.0% less  $^{17,18}\text{F}$ , and  $^{17,18}\text{O}$ , and 1.4% less  $^{19}\text{F}$  than those using the GAM91 rate.

The zone by zone analysis reveals that the SF98 case produces more  $^{18}\text{F}$  than the ORNL case for the first three zones, and the GAM91 case produces more  $^{18}\text{F}$  than ORNL for only the first two zones. The ORNL  $^{17}\text{F}(p,\gamma)^{18}\text{Ne}$  rate is slightly faster than the SF98 or GAM91 rates and there is only a small difference in the depletion of  $^{17}\text{F}$  between the three cases. The slower SF98 and GAM91  $^{17}\text{F}(p,\gamma)^{18}\text{Ne}$  rates allow even more  $^{18}\text{F}$  production to occur

later, and therefore, at lower temperatures than  $^{18}\text{F}$  production in the ORNL case.

In all three cases, the network with the faster  $^{17}\text{F}(p, \gamma)^{18}\text{Ne}$  rate produces more  $^{18}\text{F}$  in the outer zones because the lower temperatures in the outer zones do not allow for significant destruction of  $^{18}\text{F}$  via  $^{18}\text{F}(p, \alpha)^{15}\text{O}$ . Thus the early surplus of  $^{18}\text{F}$  in these zones caused by the faster  $^{17}\text{F}(p, \gamma)^{18}\text{Ne}$  rate is maintained as the envelope cools. This difference in behaviour between the inner and outer zones of an individual model shows the importance of considering nucleosynthesis (and mixing) throughout the nova envelope. If the hottest zone alone was considered, an incorrect conclusion would have been drawn regarding the changes in the abundance of  $^{18}\text{F}$ .

## 5. Results for a $1.35 M_{\odot}$ ONeMg WD Nova

The hotter  $1.35 M_{\odot}$  WD nova simulation showed the greatest variation in the mass fraction patterns produced by the four rates. Comparisons between the mass fractions calculated with the ORNL and WGT88 rates show the largest changes for  $^{17}\text{O}$  (ORNL/WGT88 mass fraction = 3.8),  $^{17}\text{F}$  (2.8),  $^{18}\text{F}$  (0.36), and  $^{18}\text{O}$  (0.38) when the entire exploding envelope was considered. A more complete sample of abundance ratios are shown in Figures 5 & 6.

In the  $1.35 M_{\odot}$  model, the largest differences in nuclear production between the ORNL and WGT88 cases were exhibited in the third hottest zone because the WGT88 rate differs more from the ORNL rate at 0.437 GK, the peak temperature in this zone, than it does at 0.457 GK, the peak temperature in the hottest zone. Comparison of mass fractions synthesized in the third hottest zone shows that using the WGT88 and ORNL  $^{17}\text{F}(p, \gamma)^{18}\text{Ne}$  rates results in very large differences in the mass fractions of  $^{17}\text{F}$  (ORNL/WGT88 mass fraction ratios = 15,000) and  $^{17}\text{O}$  (14,000). As Figure 6 illustrates, the ORNL rate also produced 31 times more  $^{14}\text{C}$  and 9 times more  $^{16}\text{O}$  than the WGT88 rate in this zone. However, the production of  $^{18}\text{F}$  and  $^{18}\text{O}$  was slightly reduced.

In the case of  $^{18}\text{F}$ , a zone by zone analysis of the  $1.35 M_{\odot}$  WD nova shows that only the innermost zone produces more  $^{18}\text{F}$  when the ORNL rate is used in place of the WGT88 rate. The  $1.35 M_{\odot}$  WD is the most violent of the three novae considered here, reaching the highest peak temperature, but also expanding, and therefore cooling, the fastest of the three novae. The temperature in the hottest zone drops from .457 GK at peak to 0.01 GK in just 60 seconds compared to the 307 seconds that the hottest zone in the  $1.25 M_{\odot}$  WD model takes to drop from a peak temperature of 0.333 GK to 0.01 GK. As was the case for the innermost zone of the  $1.25 M_{\odot}$  WD nova, the ORNL case produced more  $^{18}\text{F}$  than the WGT88 case because the WGT88 case produced its  $^{18}\text{F}$  while temperatures remained

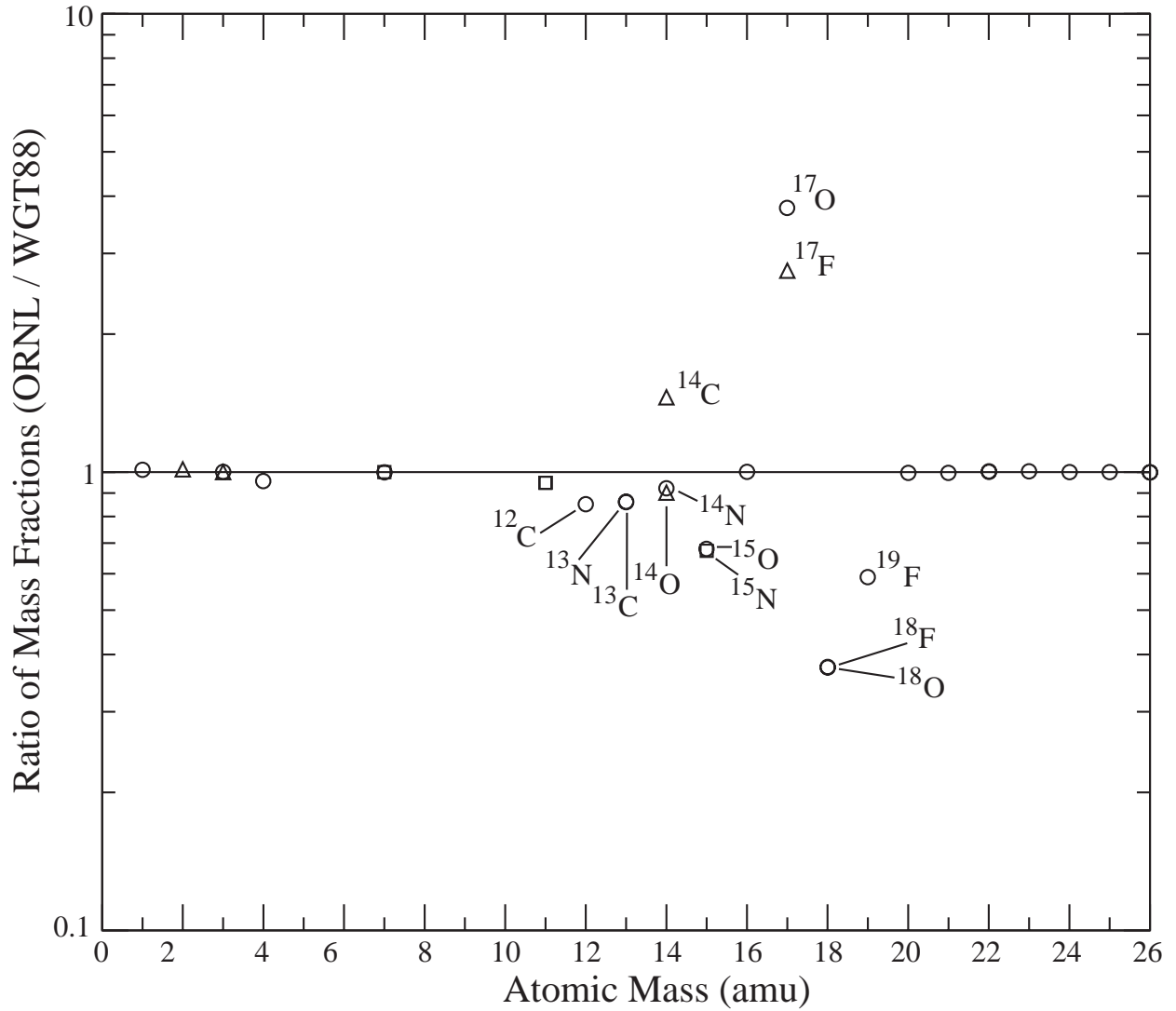


Fig. 5.— The ratio of mass fractions (ORNL/WGT88) plotted against nuclide mass for the entire envelope of a  $1.35 M_{\odot}$  WD nova. The ORNL rate changes the mass fractions of some nuclei by up to a factor of 3.8. The different symbols represent the same abundance levels as in Figure 2.

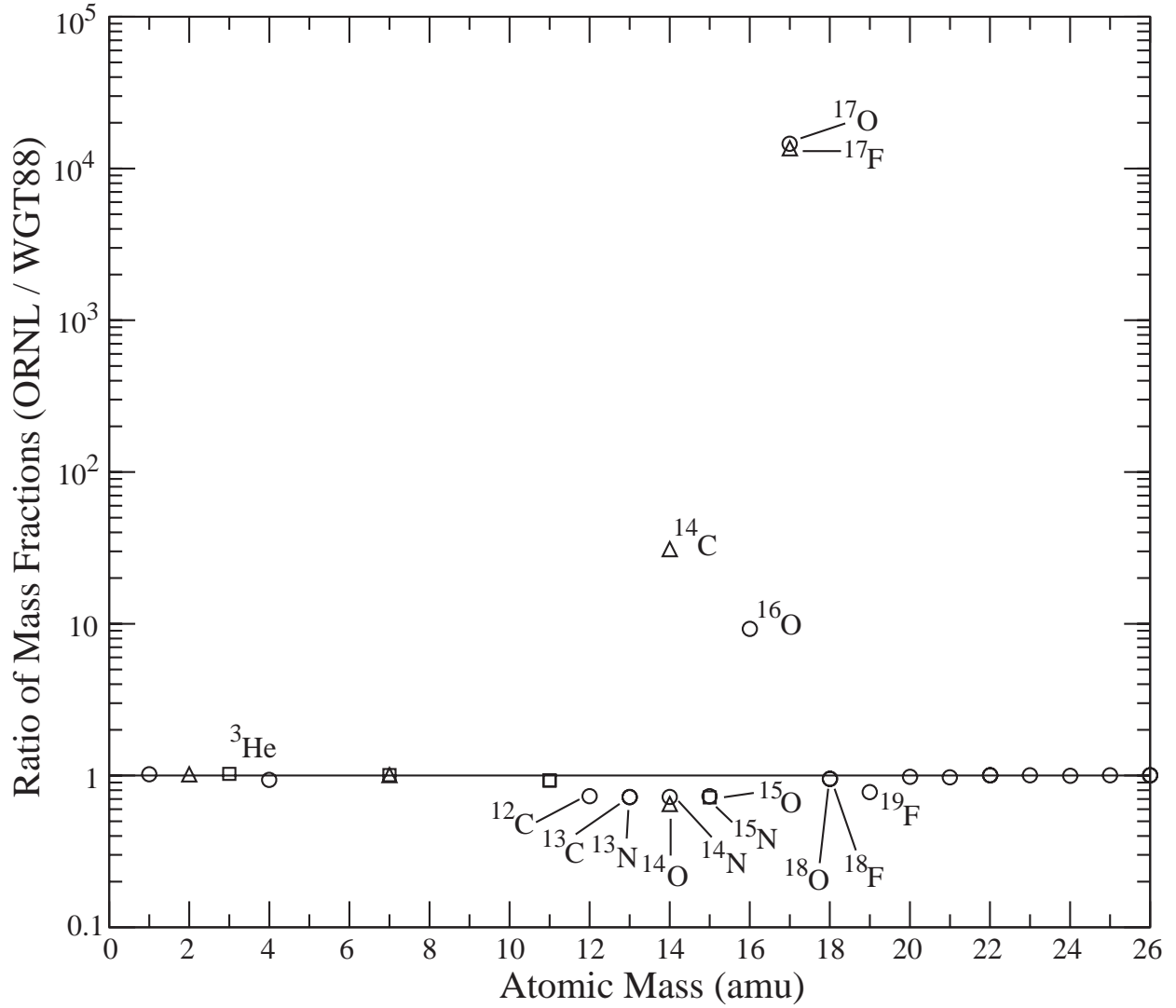


Fig. 6.— The ratio of mass fractions (ORNL/WGT88) plotted against nuclide mass for the third hottest zone of the  $1.35 M_{\odot}$  WD nova. The ORNL rate changes the mass fractions of some nuclei by up to a factor of 15000. The different symbols represent the same abundance levels as in Figure 2.

high enough for the  $^{18}\text{F}$  to be destroyed via  $^{18}\text{F}(p,\alpha)^{15}\text{O}$ . For the rest of the ejecta, the early excess in  $^{18}\text{Ne}$  and  $^{18}\text{F}$  production using the WGT88 rate is maintained because of the very rapid drop in temperature, limiting the later  $^{18}\text{F}$  destruction via the  $(p,\alpha)$  reaction. The final result is a smaller abundance of  $^{18}\text{F}$  from the ORNL rate than from the WGT88 rate (Figure 5).

As with the  $1.25 M_{\odot}$  WD nova, there were much smaller differences in mass fractions produced using the ORNL rate and the SF98 and GAM91 rates. In the SF98 and GAM91 cases the hottest zone showed the largest differences from the ORNL case because the SF98 and GAM91 rates differ more from the ORNL rate at temperatures above 0.47 GK rather than below it (see Figure 1). In the comparison with the SF98 case, when the entire exploding envelope was considered, the ORNL case resulted in 16% less  $^{14}\text{C}$ , 5% more  $^{18}\text{O}$  and  $^{18}\text{F}$ , 5% less  $^{17}\text{O}$ , and 3% less  $^{17}\text{F}$ ; all other changes were smaller. For the hottest zone, the largest change was a 66% decrease in  $^{17}\text{F}$  and  $^{17}\text{O}$  using the ORNL rate rather than the SF98 rate. In comparison with the GAM91 case, when the entire exploding envelope was considered, the ORNL case produced 3% more  $^{18}\text{F}$  and  $^{18}\text{O}$ , 2% more  $^{19}\text{F}$ , 9% less  $^{14}\text{O}$ , 3% less  $^{17}\text{O}$ , and 2% less  $^{17}\text{F}$ . The ORNL case produced about 48% less  $^{17}\text{F}$ , and  $^{17}\text{O}$ , and 12% less  $^{16}\text{O}$  than the GAM91 case in the hottest zone; all other changes were smaller.

## 6. Results for a $1.00 M_{\odot}$ CO WD Nova

Because of the lower peak temperatures, the  $1.00 M_{\odot}$  WD nova simulations showed the least variation in the abundance patterns produced by the four rates. The largest variation was in the mass fraction of  $^{18}\text{Ne}$ : 21% more  $^{18}\text{Ne}$  was produced using the WGT88 rate when compared to the ORNL case, both for the hottest zone and for the weighted sum of all zones. There was less than 0.3% change in the mass fractions of all other isotopes when comparing calculations using the ORNL and WGT88 rates. The ORNL rate resulted in 1.8% more  $^{18}\text{Ne}$  than the SF98 rate and 1.0% more  $^{18}\text{Ne}$  than the GAM91 rate in both the hottest zone and weighted average of all zones. There was less than 0.4% variation in the mass fractions of all other isotopes between the different rate cases.

## 7. Comparison with Observations and Other Studies

Novae introduce large quantities of gas and dust into the interstellar medium, and this material can be preserved in meteorites that fall to Earth. Five meteoritic dust grain inclusions have recently been shown to have isotopic signatures matching those predicted for

ONeMg nova ejecta (Amari et al. 2001a,b). Compared to solar abundances, these grains are characterized by low  $^{12}\text{C}/^{13}\text{C}$  and  $^{14}\text{N}/^{15}\text{N}$  abundance ratios, a high  $^{26}\text{Al}/^{27}\text{Al}$  abundance ratio, and large excesses of  $^{30}\text{Si}$ . Theoretical nucleosynthesis calculations show that novae ejecta are the only stellar sources that match this isotopic composition (Amari et al. 2001a,b).

Our calculated abundance ratios compare relatively well with those measured in the grains, as well as those in other nucleosynthesis calculations. The isotopic ratio of  $^{12}\text{C}/^{13}\text{C}$  for solar composition is 89.9 (Anders & Grevesse 1989), while for the five meteoritic dust grains this ratio ranges from 4 to 9.4 (Amari et al. 2001a,b). Our 1.25  $M_{\odot}$  and 1.35  $M_{\odot}$  ONeMg WD nova models predict  $^{12}\text{C}/^{13}\text{C}$  ratios of 3.2 and 5.6 respectively, while nucleosynthesis calculations from other studies predict ratios between 0.3 and 3 for ONeMg nova ejecta (Amari et al. 2001a,b; José et al. 1999). The lower limit of the  $^{26}\text{Al}/^{27}\text{Al}$  ratio was determined to be 0.8 for one of the meteoric dust grains and the ratio for another was 0.0114. Our study predicted that the ratio would be 0.15 and 0.03 for the 1.25  $M_{\odot}$  and 1.35  $M_{\odot}$  ONeMg WD nova models, respectively. Other nucleosynthesis studies predicted a ratio between 0.07 and 0.7 (Amari et al. 2001a,b; José et al. 1999). The agreement is not universally good, however. The  $^{14}\text{N}/^{15}\text{N}$  ratios are between 5.22 and 19.7 for 4 of the 5 meteoritic grains, while our study predicts ratios of 0.06 and 0.51 for the 1.25 and 1.35  $M_{\odot}$  ONeMg WD nova models, respectively. By comparison, the solar composition ratio for  $^{14}\text{N}/^{15}\text{N}$  is 270 (Anders & Grevesse 1989), so both the meteorite value and our prediction show a significant depletion in  $^{14}\text{N}$  compared to solar. Other nucleosynthesis studies predict a nitrogen isotopic ratio overlapping with ours – between 0.1 and 10 (Amari et al. 2001a,b). These comparisons show that the isotopic ratios determined from our 1.25 and 1.35  $M_{\odot}$  WD novae nucleosynthesis calculations qualitatively match those measured in grains thought to originate in novae, but further study of the impact of nuclear uncertainties on nova nucleosynthesis is certainly warranted.

Novae are thought to overproduce  $^{17}\text{O}$  and  $^{18}\text{O}$  abundances relative to solar, and the new  $^{17}\text{F}(p,\gamma)^{18}\text{Ne}$  reaction rate has a strong influence on the predicted synthesis of these isotopes. The new ORNL  $^{17}\text{F}(p,\gamma)^{18}\text{Ne}$  rate significantly changes the predictions of these isotopic abundances compared to the rate based on the resonance parameters in (Wiescher et al. 1988). Unfortunately, no oxide grains of putative novae origin have yet been identified. The discovery and analysis of oxide grains from novae would provide an important constraint on models of nova nucleosynthesis.

## 8. Summary

The abundances of certain nuclides synthesized in nova explosions on 1.25 and 1.35  $M_{\odot}$  ONeMg white dwarfs have been shown to depend strongly on the rate of the  $^{17}\text{F}(p,\gamma)^{18}\text{Ne}$  reaction. A new, slower rate for this reaction, based on a measurement with a  $^{17}\text{F}$  radioactive beam at ORNL, significantly changes the abundance predictions for  $^{17}\text{O}$  and  $^{17}\text{F}$  synthesized in the hottest zones of the explosion on a 1.35  $M_{\odot}$  WD by up to factor of 14,000 compared to predictions using a  $^{17}\text{F}(p,\gamma)^{18}\text{Ne}$  reaction rate based on resonance parameters employed in the most widely-used rate library. The new rate also changes the production of several isotopes ( $^{12,13,14}\text{C}$ ,  $^{13,14,15}\text{N}$ ,  $^{15,17,18}\text{O}$ , and  $^{17,18,19}\text{F}$ ) by as much as a factor of 3.7 when entire ejected envelope is considered. The calculations for a 1.25  $M_{\odot}$  WD nova show that this new rate changes the abundances of  $^{17,18}\text{O}$  and  $^{17,18}\text{F}$  synthesized in the hottest zones up to a factor of 600 compared to some previous estimates, and changes the abundances of  $^{12,13,14}\text{C}$ ,  $^{13,14,15}\text{N}$ ,  $^{15,17,18}\text{O}$ , and  $^{17,18,19}\text{F}$  by up to a factor of 2.1 when averaged over the entire exploding envelope. For 1.00  $M_{\odot}$  CO WD nova nucleosynthesis calculations, the peak temperatures are low enough that the values of the  $^{17}\text{F}(p,\gamma)^{18}\text{Ne}$  reaction rate differ only slightly, causing only small differences in the nucleosynthesis.

Regarding the production of the important, long-lived radionuclide  $^{18}\text{F}$ , we find that the production is increased in the hottest regions of the nova by the slower ORNL  $^{17}\text{F}(p,\gamma)^{18}\text{Ne}$  rate. A faster  $^{17}\text{F}(p,\gamma)^{18}\text{Ne}$  rate creates  $^{18}\text{F}$  (from decay of  $^{18}\text{Ne}$ ) sooner after the peak of the outburst and therefore at higher temperatures – where it is more likely to be destroyed by  $^{18}\text{F}(p,\alpha)^{15}\text{O}$ . The slower  $^{17}\text{F}(p,\gamma)^{18}\text{Ne}$  rate slows the production of  $^{18}\text{F}$ , creating more of it at a lower temperature, where it is more likely to survive as a mass 18 isotope. This effect does not, however, carry over to the outer zones of the explosion, because the overall lower temperatures of these zones limits the post-peak destruction of freshly-synthesized  $^{18}\text{F}$ . If only the innermost zones were considered, an incorrect conclusion would be drawn regarding the change in the synthesis of  $^{18}\text{F}$  – showing the importance of considering the nucleosynthesis throughout the entire nova envelope. Our predicted isotopic ratios qualitatively agree with those measured in grains from nova ejecta, as well as with other nova nucleosynthesis calculations.

Our study shows the importance of using the best nuclear physics input for calculations of the nucleosynthesis occurring in nova explosions. Even though the reaction network involves hundreds of highly-coupled reactions, an improvement to the estimate of an individual reaction rate can make a significant changes in element synthesis predictions, some of which may be directly observable through  $\gamma$ -ray astronomy or the study of presolar grains. Our results also show the strong sensitivity that nucleosynthesis calculations have to hydrodynamic profiles. With improved nuclear physics input, nucleosynthesis calculations can begin

to differentiate between competing hydrodynamic simulations of nova outbursts.

The authors acknowledge helpful comments on the manuscript from R. Kozub and the anonymous referee. Oak Ridge National Laboratory is managed by UT-Battelle, LLC, for the U.S. Department of Energy under contract DE-AC05-00OR22725. This work has been partly supported by NASA under contract NAG5-8405, by the National Science Foundation under contract AST-9877130, and by funds from the Joint Institute for Heavy Ion Research. SS acknowledges partial support from NSF and NASA grants to Arizona State Univ.

## REFERENCES

- Amari, S., Gao, X., Nittler, L. R., Zinner, E., José, J., Hernanz, M., & Lewis, R. S. 2001a, *ApJ*, 551, 1065
- Amari, S., Zinner, E., José, J., & Hernanz, M. 2001b, *Nucl. Phys. A*, 688, 430
- Anders, E. & Grevesse, N. 1989, *Geochim. Cosmochim. Acta*, 53, 197
- Bardayan, D. W., Blackmon, J. C., Brune, C. R., Champagne, A. E., Chen, A. A., Cox, J. M., Davinson, T., Hansper, V. Y., Hofstee, M. A., Johnson, B. A., Kozub, R. L., Ma, Z., Parker, P. D., Pierce, D. E., Rabban, M. T., Shotter, A. C., Smith, M. S., Swartz, K. B., Visser, D. W., & Woods, P. J. 1999, *Phys. Rev. Lett.*, 83, 45
- . 2000, *Phys. Rev. C*, 62, 055804
- Champagne, A. & Wiescher, M. 1992, *Annu. Rev. Nucl. Part. Sci.*, 42, 39
- Chin, Y., Henkel, C., Langer, N., & Mauersberger, R. 1999, *ApJ*, 512, L143
- Coc, A., Hernanz, M., José, J., & Thibaud, J.-P. 2000, *A&A*, 357, 561
- García, A., Adelberger, E. G., Magnus, P. V., Markoff, D. M., Swartz, K. B., Smith, M. S., Hahn, K. I., Bateman, N., & Parker, P. D. 1991, *Phys. Rev. C*, 43, 2012
- Gehrz, R. D., Truran, J. W., Williams, R. E., & Starrfield, S. 1998, *PASP*, 110, 3
- Gil-Pons, P., García-Berro, E., José, J., Hernanz, M. & Truran, J. W. 2003, *A&A*, in press ; astro-ph/0306197
- Harris, M. J., Naya, J. E., Teegarden, B. J., Cline, T. L., Gehrels, N., Palmer, D. M., Ramaty, R., & Seifert, H. 1999, *ApJ*, 522, 424

- Harris, M. J., Teegarden, B. J., Weidenspointner, G., Palmer, D. M., Cline, T. L., Gehrels, N., & Ramaty, R. 2001, *ApJ*, 563, 950
- Hernanz, M., Gómez-Gomar, J., José, J., & Coc, A. 2001, in *Exploring the gamma-ray universe. Proceedings of the Fourth INTEGRAL Workshop*, ed. A. Gimenez, V. Reglero, & C. Winkler (Noordwijk: ESA SP-459), 65–68
- Hernanz, M., José, J., Coc, A., Gómez-Gomar, J., & Isern, J. 1999, *ApJ*, 526, L97
- Hix, W. R. & Thielemann, F.-K. 1999, *J. Comp. Appl. Math*, 109, 321
- José, J., Coc, A., & Hernanz, M. 1999, *ApJ*, 520, 347
- Kercek, A., Hillebrandt, W., & Truran, J. W. 1999, *A&A*, 345, 831
- Leising, M. D. & Clayton, D. D. 1987, *ApJ*, 323, 159
- Politano, M., Starrfield, S., Truran, J. W., Weiss, A., & Sparks, W. M. 1995, *ApJ*, 448, 807
- Shankar, A. & Arnett, D. 1994, *ApJ*, 433, 216
- Sherr, R. & Fortune, H. T. 1998, *Phys. Rev. C*, 58, 3292
- Starrfield, S. 1989, in *Classical Novae*, ed. M. Bode & A. Evans (Wiley:Chichester), 39–60
- Starrfield, S., Sparks, W. M., & Truran, J. W. 1974, *ApJS*, 28, 247
- Starrfield, S., Truran, J. W., & Sparks, W. M. 1978, *ApJ*, 226, 186
- Starrfield, S., Truran, J. W., Wiescher, M. C., & Sparks, W. M. 1998, *MNRAS*, 296, 502
- Thielemann, F.-K., Freiburghaus, C., Rauscher, T., et al. 1995, [ie.lbl.gov/astro/friedel.html](http://ie.lbl.gov/astro/friedel.html)
- Van Wormer, L., Goerres, J., Iliadis, C., Wiescher, M., & Thielemann, F.-K. 1994, *ApJ*, 432, 326
- Vanlandingham, K. M., Starrfield, S., Wagner, R. M., Shore, S. N., & Sonneborn, G. 1996, *MNRAS*, 282, 563
- Wallace, R. K. & Woosley, S. E. 1981, *ApJS*, 45, 389
- Wanajo, S., Hashimoto, M.-A., & Nomoto, K. 1999, *ApJ*, 523, 409
- Wiescher, M., Gorres, J., & Thielemann, F. 1988, *ApJ*, 326, 384
- Wiescher, M., Schatz, H., & Champagne, A. 1998, *Phil. Trans. R. Soc. Lond. A*, 356, 2105

